

NASDUCK SERF: New constraints on axion-like dark matter from a SERF comagnetometer

Itay M. Bloch,^{1,2} Roy Shaham,^{3,4} Yonit Hochberg,⁵ Eric Kuflik,⁵ Tomer Volansky,⁶ and Or Katz^{7,8,*}

¹*Berkeley Center for Theoretical Physics, University of California, Berkeley, CA 94720, U.S.A.*

²*Theory Group, Lawrence Berkeley National Laboratory, Berkeley, CA 94720, U.S.A.*

³*Rafael Ltd., 31021 Haifa, Israel*

⁴*Department of Physics of Complex Systems, Weizmann Institute of Science, Rehovot 76100, Israel*

⁵*Racah Institute of Physics, Hebrew University of Jerusalem, Jerusalem 91904, Israel*

⁶*Department of Physics, Tel Aviv University, Tel Aviv, Israel*

⁷*Duke Quantum Center, Duke University, Durham, NC 27701*

⁸*Department of Electrical and Computer Engineering, Duke University, Durham, NC 27708*

Ultralight axion-like particles are well-motivated relics that might compose the cosmological dark matter and source anomalous time-dependent magnetic fields. We report on new terrestrial bounds on the coupling of axion-like particles to neutrons and protons. The detector uses nuclei of noble-gas and alkali-metal atoms and operates in the Spin-Exchange Relaxation-Free (SERF) regime, achieving high sensitivity to axion-like dark matter fields. Conducting a month-long search, we cover the mass range of $1.4 \times 10^{-12} \text{ eV}/c^2$ to $2 \times 10^{-10} \text{ eV}/c^2$ and provide world-leading limits which supersede robust astrophysical bounds, and improve upon previous terrestrial constraints by up to two orders of magnitudes for many masses within this range. These are the first reliable terrestrial bounds reported on the coupling of protons with axion-like dark matter, covering a new and unexplored terrain in its parameter space.

I. INTRODUCTION

It has been known for nearly a century that most of the matter in our universe is non-luminous. The presence of this so called Dark Matter (DM) has been confirmed by a wide range of observations on all scales. However, to date, all observations rely on the DM's gravitational interactions, precluding the determination of its particle identity, including its mass and interactions. A highly motivated and well-studied class of DM candidates are Axion-Like Particles (ALPs) in the ultralight mass regime [1, 2]. Originally introduced to solve the strong CP problem of the Standard Model of particle physics [3–5], the axion and its generalizations can explain the observed DM relic abundance, and at the same time, predict feeble non-gravitational interactions with visible matter which can be probed experimentally [1].

ALPs may interact with gluons or photons, or with fermions such as protons, neutrons and electrons. Various experiments explore constraints on these possible couplings of the ALP DM [6–8]. Most classical direct detection experiments search for DM from masses at the eV/c^2 scale and above via absorption by or scattering from target materials [9]. While ultralight ALPs cannot be detected using such techniques, significant progress has been made recently in the search for them using experiments on earth [10–21]. For light enough ALPs, the predicted density is high enough so that it can be treated as a classical background field which may be detectable by other means. In particular, when interacting with fermions, the ALP exhibits itself as a

coherent narrow-bandwidth *time-dependent*, *anomalous* field which interacts with the spins of target fermions [22].

Atomic magnetometers, Nuclear Magnetic Resonance (NMR) sensors and co-magnetometers are terrestrial detectors which are utilized for the search of ALP-sourced anomalous fields and other signatures of physics beyond the Standard Model [11, 12, 17–19, 21, 24–31]. These sensors use spin-polarized atoms in a gaseous, liquid, or solid phase which collectively respond to the anomalous-magnetic field of the ALP and can thus detect or constrain the couplings of ALP to fermions. Typically, the mass range in these searches is set by the relaxation rate of the spins and their resonance frequencies, which determine the range in which the spins are most sensitive to oscillating fields.

Previous searches have utilized dual atomic species to search for ALP DM at small masses, usually using nuclear spins as at least one of the species [12, 19, 21, 24, 32, 33]. They relied on simultaneous overlapping of the resonance frequencies of the two species at the oscillating frequency of the ALP, which limited the measurement bandwidth to $f \lesssim 1 \text{ Hz}$ (about $4 \times 10^{-15} \text{ eV}/h$). Owing to the limited search duration (typically up to several months), previous bounds were cast on $m_{\text{DM}} \lesssim 4 \times 10^{-12} \text{ eV}/c^2$ [11, 32, 34]. To constrain higher ALP masses one may focus on the response of ALPs at a single broadband resonance and operate in the SERF regime [35–37] to suppress non-magnetic noise sources. While several techniques have been proposed previously [38], to this day none has been directly implemented above $m_{\text{DM}} > 4 \times 10^{-14} \text{ eV}/c^2$ [32].

Furthermore, the most stringent terrestrial constraints of the coupling between ALPs and fermions in the ultralight mass regime are based on atomic detectors that use nuclear spins of noble gases. These spins are composed predominantly by their valence neutrons, which enables

* or.katz@duke.edu

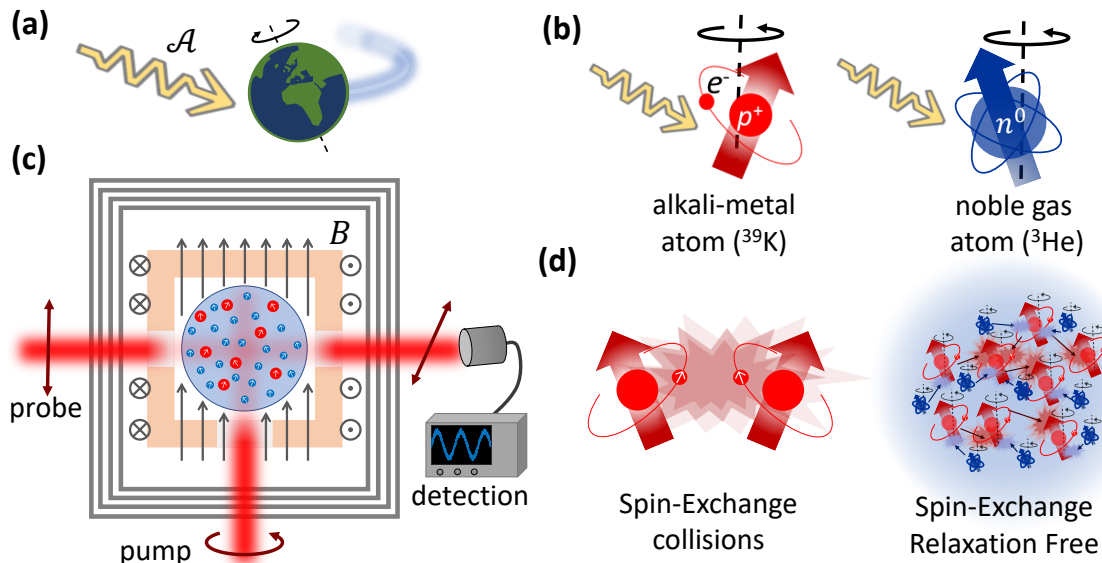


FIG. 1. **Search for ALP dark matter using a SERF comagnetometer.** (a) As the Earth moves through the dark matter halo, matter on Earth can potentially interact with the Axion-Like Particles (ALPs) dark matter in a non-gravitational manner. Such interactions can manifest through the gradient field $\mathcal{A} = \nabla a$ of the ALP coupling to other particles. (b) ALPs coupling to atoms. The coupling to alkali-metal and noble-gas nuclear spins is manifested as an anomalous-magnetic field which drives the precession of the spins. The coupling to noble-gas spins is predominantly through their valence neutron whereas the coupling to alkali-metal nuclei is predominantly through their proton hole in their nucleus [23]. (c) Detector configuration. Spin-polarized ^{39}K (red) and ^3He (blue) gases are contained in a spherical glass cell, and their precession at a constant magnetic field B is optically monitored. The magnetic field determines the resonance precession frequency of the atoms and thus also the ALP masses for which the detector is sensitive. (d) Operation in SERF regime. Operation with high potassium density renders random spin-exchange collisions between pairs of ^{39}K atoms very frequent, but also suppresses their relaxation (Spin-Exchange Relaxation Free). Collisions between ^3He and ^{39}K coherently couple the spin gases and enables to superpose the signal of the ^3He on the optically measured ^{39}K .

measurable ALP-neutron interactions. However, cases where the ALP-proton interaction dominates are also theoretically motivated [39]. For instance, in models of hadronic axions (e.g. the KSVZ model [40, 41]), ALPs do not couple to quarks and leptons at high energies, and as a consequence their coupling to neutrons is small or could possibly vanish, while their coupling to protons remains sizeable [39]. Constraining the coupling between ALPs and protons requires nuclear spins whose proton contribution is large and known to a sufficient accuracy. Therefore to this day, no reliable bounds on ALP DM interaction with protons were reported in any terrestrial technique.

Here we report on new experimental constraints on ALP DM interactions with protons and neutrons. The results rely on a month long search using a dual-specie spin ensembles of polarized ^3He and ^{39}K (potassium) atoms. The former is sensitive to ALP-neutron coupling and the latter to ALP-proton coupling, utilizing the nonzero neutron or proton contributions to the spin in their nuclei. Operating the detector in the Spin-Exchange Relaxation-Free (SERF) regime with a high number-density for the potassium, we suppress the effect of photon shot noise and improve on the current terrestrial limits of the coupling to neutrons and protons by as much as two orders of magnitude in the mass range

$1.4 \times 10^{-12} - 2 \times 10^{-10} \text{ eV}/c^2$. Moreover, barring the uncertain supernova constraints, the ALP-proton bound improves on all existing terrestrial and astrophysical limits, partially closing the region for couplings in the range $5 \times 10^{-6} \text{ GeV}^{-1}$ to $2 \times 10^{-5} \text{ GeV}^{-1}$.

II. ALP INTERACTIONS WITH FERMIONS

We use a gaseous mixture of alkali-metal and noble-gas spins whose nuclear spins can couple to the ALPs as shown in Fig. 1. The interaction Hamiltonian of ALP fields with noble-gas spins is given by

$$H_{\text{ALP-He}} = g_{\text{N}} \mathcal{A} \cdot \mathbf{N} \quad (1)$$

where $\mathbf{N} = \sum_n \mathbf{N}_n$ is the collective nuclear spin operators of the noble-gas ensemble, summing over the operators of all noble-gas spins in the measurement volume. The vector $\mathcal{A} = \nabla a$ denotes the gradient of the ALP field a , which is a stochastic variable whose spectral content depends on the energy density and the velocity distribution of DM \mathbf{v}_{DM} [42], and is concentrated in a narrow band of frequencies near $\omega_{\text{DM}} = (m_{\text{DM}}c^2 + \langle \mathbf{v}_{\text{DM}}^2 \rangle / 2) / \hbar$. The factor g_{N} represents the coupling between ALPs and the particles that compose

the nuclear spin. For ${}^3\text{He}$ (spin 1/2), the dominant contribution comes from its single valence neutron, such that $g_N = \epsilon_N g_{aNN}$. We take $\epsilon_N \approx 0.85$ for the fractional contribution of neutron spin to the nuclear spin of ${}^3\text{He}$ atoms [43]. g_{aNN} is the ALP-neutron coupling coefficient we aim to bound.

We use spins of alkali-metal atoms to detect the Helium response as an optical SERF magnetometer, and concurrently, to constrain the coupling between ALPs and protons as illustrated in Fig. 1b. ${}^{39}\text{K}$ atoms have a single valence electron (spin-1/2) as well as a nonzero nuclear spin. The interaction Hamiltonian of ALP fields with alkali-metal nuclei is given by

$$H_{\text{ALP-K}} = g_{\text{I}} \mathcal{A} \cdot \mathbf{I}. \quad (2)$$

Here $\mathbf{I} = \sum_i \mathbf{I}_i$ denotes the collective nuclear spin operator of the alkali-metal atoms, summing over all alkali-metal atoms in the measurement volume. We use natural abundant potassium atoms (predominantly ${}^{39}\text{K}$ with spin-3/2) which have a proton hole that dominates the nuclear spin [23]. We then cast $g_{\text{I}} = \epsilon_{\text{P}} g_{aPP}$ where $\epsilon_{\text{P}} \approx 0.16 \pm 0.04$ is the fractional contribution of proton spin to the nuclear spin for ${}^{39}\text{K}$ where the uncertainty denotes the spread of prediction by the models reviewed in Ref. [23]. These models also report on uncertain and much smaller fractional contribution of neutron spin, which is consistent with or is exactly zero; in this search we neglect this contribution. g_{aPP} is the ALP-proton coupling coefficient we aim to bound.

III. SEARCHING FOR NEW PHYSICS WITH SERF MAGNETOMETERS

A. Apparatus

The detector is comprised of a naturally abundant potassium vapor and 1500 Torr of ${}^3\text{He}$ gas that are enclosed in a spherical glass cell¹ as shown in Fig. 1c. The two spin ensembles are initially unpolarized; we orient the spins by continuous optical-pumping of the potassium spins, reaching a polarization degree of $P_{\text{K}} \approx 85\%$. Subsequently, the helium spins are polarized by collisions with the optically-pumped potassium atoms, in a process known as spin-exchange optical-pumping (SEOP) [55], reaching a polarization degree of $P_{\text{He}} \approx 20\%$. The spins are aligned along an externally applied magnetic field $B_z \hat{z}$ and are magnetically shielded from the ambient field. The magnetic field together with applied light-shifts and the spin-exchange shifts generated by the two polarized spin gases determine the electron paramagnetic resonance (EPR) frequency ω_{K} of the potassium spins

and the nuclear magnetic resonance (NMR) frequency ω_{He} of the helium spins. We use an off-resonant optical probe to measure the collective total spin of the alkali-metal atoms along the \hat{x} direction via polarimetry technique, using a pair of photo-diodes in a homodyne configuration [56].

We operate the detector in the SERF regime, for which relaxation by spin-exchange collisions between alkali-metal pairs and also by spin-destruction collisions is highly suppressed [37, 57–60]. This regime is realized by using an elevated potassium density for which the EPR frequencies we consider are much slower than the rapid rate of spin-exchange collisions $R_{\text{SE}} \approx 5 \times 10^5 \text{ s}^{-1}$. It allows us to use a large number of potassium atoms $N_{\text{K}} \approx 5 \times 10^{14}$ to increase the apparatus sensitivity, yet maintain a low decoherence rate; e.g. at $\omega_{\text{K}} = 10 \text{ kHz}$, the measured magnetic decoherence rate² is $\Gamma_{\text{K}} = 770 \text{ Hz}$, about three orders of magnitudes smaller than R_{SE} . The sensitivity of the apparatus to magnetic or anomalous fields oscillating near the EPR resonance is better than $\sim 2 \text{ fT}/\sqrt{\text{Hz}}$, but at most search frequencies, the sensitivity to anomalous fields is dominated by a magnetic-field noise floor of about $10 \text{ fT}/\sqrt{\text{Hz}}$ (see Methods).

B. Response to ALP field

We can describe the response of the collective spins of the alkali-metal and noble-gas spins to the ALP field with the Bloch-equations. A weak oscillatory field in the xy plane $\mathcal{A}_+ = \mathcal{A}_x + i\mathcal{A}_y$ exerts a torque that rotates the orientation of the collective spins of the two gases off the \hat{z} axis, and generates a steady precession. The response of the spins depends on the amplitude of the ALP field and on the frequency difference of ω_{DM} from their magnetic resonance. Anomalous fields that couple to neutrons tilt the helium spins and produce an oscillating spin component with amplitude

$$\langle N_+ \rangle = \frac{P_{\text{He}} N_{\text{He}}}{2} \frac{g_{\text{N}} \mathcal{A}_+}{\omega_{\text{He}} - \omega_{\text{DM}} - i\Gamma_{\text{He}}}. \quad (3)$$

Here $\langle N_+ \rangle = \langle N_x \rangle + i\langle N_y \rangle$ denotes the mean collective spin of the helium ensemble in the transverse direction and $\Gamma_{\text{He}} < 0.1 \text{ Hz}$ is the spin decoherence rate. In our search range $\omega_{\text{DM}} \gg \omega_{\text{He}} \gg \Gamma_{\text{He}}$.

Owing to the great separation between the EPR and NMR resonances considered in this search ($\omega_{\text{DM}}, \omega_{\text{K}} \gg \omega_{\text{He}}$) the dynamics of the two spin gases is weakly-coupled [54, 61–63]. Consequently, the total collective spin of the potassium $\langle \mathbf{F} \rangle = \sum_i (\langle \mathbf{I}_i \rangle + \langle \mathbf{S}_i \rangle)$, comprised of summation over the potassiums' nuclear and electron spins, simultaneously responds to the torque exerted by

¹ The cell also contains 40 Torr of N_2 gas to mitigate radiation trapping and assist the optical pumping process. Further details on the apparatus are given in Ref. [54].

² This is the total decoherence rate including power broadening by continuous optical-pumping, residual spin-exchange relaxation and other relaxation processes.

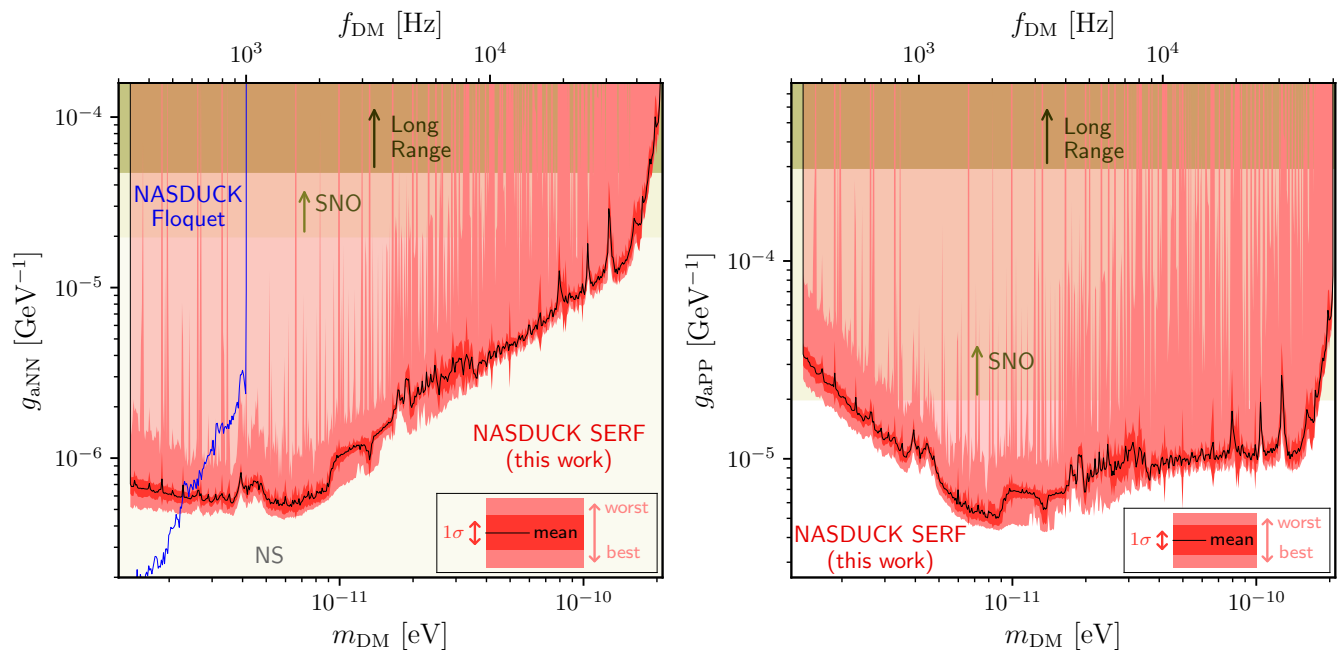


FIG. 2. **Constraints on ALP-neutron and ALP-proton couplings.** In this work we use a NASDUCK collaboration SERF comagnetometer to constrain ALP couplings over a broad range of ALP masses. We present 95% C.L. limits. The **light transparent red region** shows the exclusion region for the ALP-neutron couplings (*left*) and ALP-proton couplings (*right*). Due to the finite resolution of the figure and given the dense set of measurements, the limits appear as a **bright red band**. The width of this band denotes the strongest and weakest values around each mass point. The precise tabulated bounds can be found in [44]. The **black solid line** shows a binned average of the bound while its 1σ variation is shown as the **red band** (both calculated in log-log space at a binning resolution of 1% of the mass). Other terrestrial constraints from searches for long-range forces (which do not search for dark matter) [25, 45] (**olive-green** region) and from NASDUCK-Floquet [11] (**blue-line**) are presented. In **beige** we depict the excluded regions from solar ALPs unobserved at the Solar Neutrino Observatory (SNO) [46]; for the neutron couplings in the left panel, we also show the complementary stellar constraints from neutron stars cooling [47–50] (exceeding the scale of the figure). We do not show the model-dependent limits from supernova (SN) cooling considerations and neutrino flux measurements [1, 51, 52], which would constrain the entire range presented in the figure, since they notably rely on the unknown SN collapse mechanism [53].

the precessing helium and by its direct coupling to the ALP. Representing the collective spin of the alkali-metal vapor in a complex form $\langle F_+ \rangle = \langle F_x \rangle + i\langle F_y \rangle$, we derive the total spin response to ALP fields

$$\langle F_+ \rangle = \frac{P_K N_K}{2} \frac{(\zeta g_{aPP} - \xi g_{aNN}) \mathcal{A}_+}{\omega_K - \omega_{DM} - i\Gamma_K}, \quad (4)$$

where the unitless parameter ξ depends inversely on ω_{DM} and varies in the search between 46 at low frequencies to 0.29 at high frequencies and $\zeta = 0.69$ (see Methods). The potassium spin component $\langle F_x \rangle$ is directly detected by the optical probe, allowing to simultaneously measure g_{aPP} and g_{aNN} .

IV. THE SEARCH

A. Data acquisition

We searched for ALP fields with f_{DM} in the range of 0.33 – 50 kHz (corresponding to a mass range of 1.4 to

200 peV/ c^2) by recording the precession of the potassium in the absence of any applied oscillating fields. We varied the magnetic field at few tens of discrete points, and at each point recorded the detector’s response for a duration that is longer than the coherence time of the ALP and is about $10^7 - 10^8$ oscillations of the EPR frequency at that field. Over a one-month period, we completed 5 different scans with different samplings of the magnetic field in the range $B_z = 10 - 70$ mG to gain sensitivity for ALP fields that oscillate in the reported search range. Each measurement was preceded by initial pumping of the helium spins at $B_z = 70$ mG, and was preceded and appended by a calibration of the magnetic response and the helium spin polarization. The first and fourth scans were designated to optimize the analysis procedure and were not used to cast bounds, as was decided before unblinding.

B. Search results

We use the log-likelihood ratio test to constrain the presence of ALP DM with 95% confidence level (C.L.) bounds, presented in Fig 2 for the ALP-neutron coupling (*left*) and ALP-proton coupling (*right*). The stochastic nature of the ALPs was treated using the method of Ref. [11] (see also Refs. [10, 26, 64] for similar procedures). The search only aims to exclude ALPs and does not attempt at a possible discovery. These constraints cover the mass range between $1.4 \text{ peV}/c^2$ and $200 \text{ peV}/c^2$, measured with a resolution slightly higher than the line-width of the ALP wavepacket (about $3 \times 10^{-7} m_a$ taking m_a as the ALP mass). While the entire bounds as a function of mass is tabulated in Ref. [44], we illustrate the limits by their geometric mean in log-spaced bins of size 1% of the mass (black lines), surrounded by the standard deviation (computed in log-space) spread of bounds in the same bins (red), further surrounded by the minimal and maximal bounds found in each bin (bright red). All couplings above the bright red bands are excluded (light transparent red region).

The olive green regions show constraints from other long-range searches on ALP-neutron [25] and ALP-proton [45] couplings (which do not search for dark matter). The blue line is the mean exclusion line of the NASDUCK-Floquet experiment [11]. Our results provide complementary probes to stellar constraints. The beige regions come from searches for ALP-emission from the sun by the Solar Neutrino Observatory [46] and from neutron star (NS) cooling considerations [47–50]. The latter extends throughout the entire plotted region of the ALP-neutron coupling. For both neutron and proton couplings, the shown regions are constrained by model-dependent supernova (SN) cooling considerations or neutrino flux measurements from SN1987A [1, 51, 52]. Since the theoretical reliability of such limits is arguable due to the unknown SN collapse mechanism [53], we do not plot them here. The newly derived limits of this search, dubbed NASDUCK-SERF, on the ALP couplings to neutrons, improve the existing terrestrial limits over nearly the entire mass range by up to two orders of magnitude, providing a strong complementary probe to stellar constraints from NS and SN. Furthermore, our bound on ALP-protons interactions in a large part of the mass range from $2 \text{ peV}/c^2$ to $100 \text{ peV}/c^2$ lies in a region that is otherwise only excluded by model-dependent arguable SN constraints.

V. DISCUSSION AND OUTLOOK

It is interesting to compare the operation and sensitivity of our detector with self-compensating co-magnetometers that hold the strongest terrestrial bounds on neutron coupling at low frequencies [12, 65, 66]. Self-compensating co-magnetometers use similar mixtures of alkali-metal and noble-gas spins to detect anomalous

fields but set the EPR frequency ω_K near resonance with the NMR frequency ω_{He} to realize damped and near-critically coupled dynamics. This operation enhances the signal to noise ratio for detecting oscillating anomalous fields that act on the noble-gas spins at very low frequencies below $\omega_{\text{DM}} \lesssim 10 \text{ Hz}$, by suppressing magnetic noises [67]. However, for the range of ALP frequencies that we consider in this work, $\omega_{\text{DM}} \gg \omega_{\text{He}}$ such that the low-frequency enhancement and suppression mechanisms are rendered ineffective, and neither the alkali-metal nor the noble-gas spins are resonant with the driving field. Our detector instead, sets the EPR resonance near the frequency of the searched ALP, and by that fully exploits the high sensitivity of the SERF magnetometer. This operation therefore improves the sensitivity to anomalous fields by about a factor of $\omega_{\text{DM}}/\Gamma_K$ compared to self-compensating co-magnetometers, which is more than 100-fold at the high-frequency end of our search range.

The constraints set by our search are predominantly limited by the magnetic field noise that is produced by our innermost magnetic shield layer. Replacement of this layer by a low-noise material (e.g. MnZn ferrite [68]) is expected to reduce the magnetic noise level by a factor of $\mathcal{O}(5)$. Furthermore, it is possible to improve the bounds on neutrons by using a denser noble-gas and hybrid SEOP, which are expected to further improve the noble-gas spin magnetization.

ACKNOWLEDGMENTS

Acknowledgments. The work of YH is supported by the Israel Science Foundation (grants No. 1112/17 and 1818/22), by the Binational Science Foundation (grant No. 2016155), by the Azrieli Foundation and by an ERC STG grant (grant No. 101040019). EK is supported by the US-Israeli Binational Science Foundation (grant No. 2020220) and by the Israel Science Foundation (grant No. 1111/17). TV is supported by the Israel Science Foundation (grant No. 1862/21), by the Binational Science Foundation (grant No. 2020220) and by the European Research Council (ERC) under the EU Horizon 2020 Programme (ERC-CoG-2015 - Proposal n. 682676 LDMThExp). This project has received funding from the European Research Council (ERC) under the European Union’s Horizon Europe research and innovation programme (grant agreement No. 101040019). Views and opinions expressed are however those of the author(s) only and do not necessarily reflect those of the European Union. The European Union cannot be held responsible for them.

METHODS

A. Spin dynamics in the SERF regime

The electron and nuclear spins of the potassium are coupled via the strong hyperfine interaction $H_{\text{hpf}} = A_{\text{hpf}} \mathbf{I}_i \cdot \mathbf{S}_i$, which sets the total spin in the electronic ground-state $\mathbf{F}_i = \mathbf{I}_i + \mathbf{S}_i$ of the i th atom as an operator with good quantum numbers. We can describe the dynamics of the collective spin of the potassium ensemble $\mathbf{F} = \sum_i \mathbf{F}_i$ and the helium spin ensemble $\mathbf{N} = \sum_i \mathbf{N}_i$ in the xy plane using the coupled Bloch equations [69]

$$\frac{d}{dt} \langle \mathbf{F} \rangle = - \left(\gamma_e \mathbf{B} + \frac{2qA_{\text{He}}}{N_{\text{He}}} \langle \mathbf{N} \rangle \right) \times \langle \mathbf{S} \rangle - g_{\text{I}} \mathcal{A} \times \langle \mathbf{I} \rangle - \Gamma_{\text{K}} \langle \mathbf{F} \rangle, \quad (5)$$

$$\frac{d}{dt} \langle \mathbf{N} \rangle = - \left(\gamma_{\text{N}} \mathbf{B} + \frac{2A_{\text{K}}}{N_{\text{K}}} \langle \mathbf{S} \rangle \right) \times \langle \mathbf{N} \rangle - g_{\text{N}} \mathcal{A} \times \langle \mathbf{N} \rangle - \Gamma_{\text{He}} \langle \mathbf{N} \rangle. \quad (6)$$

Here γ_e , γ_{N} are the gyro-magnetic ratios of the bare electron and helium spins respectively, and $\mathbf{B} = B_z \hat{\mathbf{z}}$ is the magnetic field. $q(P_{\text{K}})$ is the slowing-down-factor [70], monotonically decreasing from $q(P_{\text{K}} = 0) = 6$ to $q(P_{\text{K}} = 1) = 4$ as a function of P_{K} , the potassium degree of polarization. It is experimentally determined by measurement of the gyro-magnetic ratio of the potassium in our setup, giving $q = 4.3$. A_{He} (A_{K}) are the total spin-exchange shifts of the magnetic levels had all helium (potassium) spins were completely polarized, *i.e.* $|\langle \mathbf{N} \rangle| = N_{\text{He}}/2$ ($|\langle \mathbf{S} \rangle| = N_{\text{He}}/2$), and in our experiment $A_{\text{He}} \approx 18$ kHz and $A_{\text{K}} \approx 0.8$ Hz. We denote the collective spins of the electrons and nuclei of alkali-metal atoms $\langle \mathbf{S} \rangle = \sum_i \langle \mathbf{S}_i \rangle$ and $\langle \mathbf{I} \rangle = \sum_i \langle \mathbf{I}_i \rangle$. We denote by Γ_{He} and Γ_{K} the transverse relaxation rates of the helium and potassium spins respectively.

The ALP fields interacting with the alkali-metal nuclei exert a torque on the collective nuclear spin $\langle \mathbf{I} \rangle = \sum_i \langle \mathbf{I}_i \rangle$. Here we consider a dense alkali ensemble in the SERF regime, for which rapid spin-exchange collisions between pairs of alkali-metal atoms drive the spin state to follow a spin temperature distribution, and correlate the mean collective spins by $\langle \mathbf{F} \rangle = q \langle \mathbf{S} \rangle = \frac{q}{q-1} \langle \mathbf{I} \rangle$ [70]. The number of polarized atoms are $P_{\text{K}} N_{\text{K}} = 2|\langle \mathbf{S} \rangle|$ for the potassium and $P_{\text{He}} N_{\text{He}} = 2|\langle \mathbf{N} \rangle|$ for the helium [69, 71]. In our experimental setup, the spins are nearly aligned with the z direction, such that $|\langle \mathbf{S} \rangle| \approx |\langle S_z \rangle|$ and $|\langle \mathbf{N} \rangle| \approx |\langle N_z \rangle|$.

In the regime we operate the apparatus, the EPR frequency associated with the precession of the total alkali-metal spin $\omega_{\text{K}} = |\frac{1}{q} B \gamma_e + P_{\text{He}} A_{\text{He}}|$ is about two orders of magnitude larger than the NMR frequency of the helium spins $\omega_{\text{He}} = |\gamma_{\text{N}} B + P_{\text{K}} A_{\text{K}}|$. This different scaling originates from the difference in the gyromagnetic ratios, and the application of magnetic field that is aligned with spin-exchange field produced by the helium (A_{He}), in contrast with the operation of self compensating co-magnetometers which use an inverted magnetic field [63, 65]. Considering the spectral response of the helium spins to oscillating dark matter fields that are near the resonance of the potassium spins, we obtain Eq. (3) as the fourier transform of Eq. (6) after neglecting the small effect of $\langle S_{\pm} \rangle$ on the noble-gas dynamics.

The response of the transverse collective spin $\langle \mathbf{F}_{\pm} \rangle$ can similarly be represented in the frequency domain by

$$\langle \mathbf{F}_{\pm}(\omega) \rangle = \frac{P_{\text{K}} N_{\text{K}}}{2} \frac{\frac{2qA_{\text{He}}}{N_{\text{He}}} \langle \mathbf{N}_{\pm}(\omega) \rangle + g_{\text{I}}(q-1) \mathcal{A}_{\pm}(\omega)}{\omega_{\text{K}} - \omega - i\Gamma_{\text{K}}}. \quad (7)$$

Substitution of Eq. (3) in Eq. (7) directly yields Eq. (4), with the effective coupling coefficient reading

$$g_{\text{eff}} \equiv (q-1) \epsilon_{\text{P}} g_{\alpha\text{PP}} - \xi g_{\alpha\text{NN}}. \quad (8)$$

We can therefore identify the first unitless coefficient $\zeta = (q-1) \epsilon_{\text{P}} \approx 0.69$ and the second unitless coefficient as

$$\xi(\omega) = \frac{q \epsilon_{\text{N}} P_{\text{He}} A_{\text{He}}}{\omega - \omega_{\text{He}} + i\Gamma_{\text{He}}} \approx \frac{q \epsilon_{\text{N}} P_{\text{He}} A_{\text{He}}}{\omega}. \quad (9)$$

The last approximation pertains to the spectral content far from the helium resonance, because in our search range $\omega \gg \omega_{\text{He}}, \Gamma_{\text{He}}$ as ω is near ω_{K} .

B. Background and signal sensitivity

The detector is sensitive to both real and anomalous magnetic fields. In this section, we present and characterize the noise model for the detector and analyze the sources of noise that limit its detection sensitivity in most frequencies.

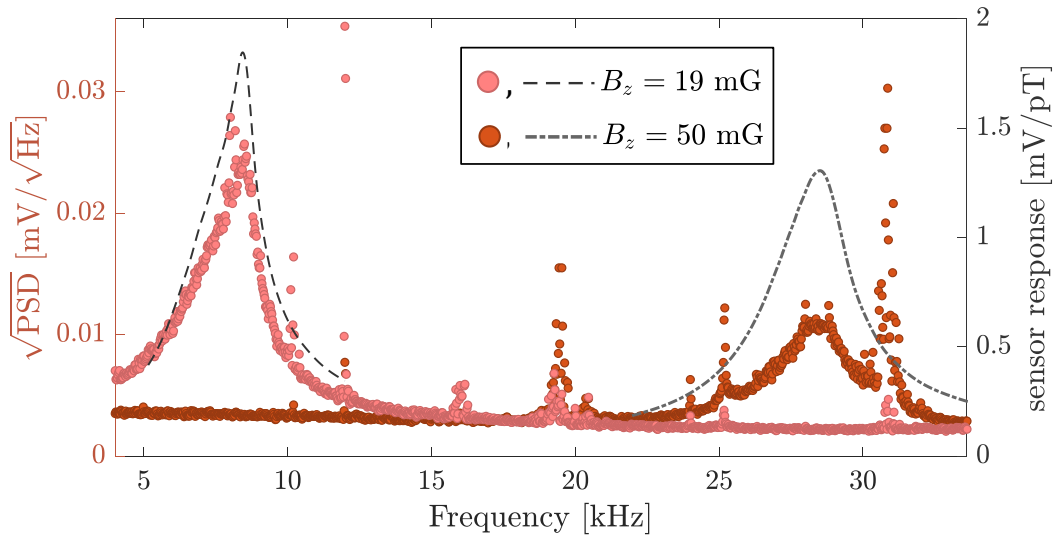


FIG. 3. **Noise spectral density and magnetic response.** Measured noise spectral density PSD of the detector (left axis) at two different magnetic fields in the search ($B_z = 19$ mG, pink circles and $B_z = 50$ mG, brown circles). Apart for some peaks, the spectrum generally follows an offset Lorentzian profile, owing to magnetic field noise and limited sensitivity of the detector. Dashed and dotted-dashed curves show the measured detector response to weakly oscillating transverse magnetic fields along the y direction for $B_z = 19, 50$ mG respectively (right axis).

The dominant sources of noise are the magnetic field noise and noise that is associated with our optical detection, primarily polarization noise of the probe beam that is associated with its shot noise.

The magnetometer signal is proportional to the collective spin component $\langle F_x \rangle = \text{Re}(\langle F_+ \rangle)$ whose response to ALPs is given in Eq. (4). In the presence of noise, the collective spin measured by the detector reads as $\langle F_+ \rangle \rightarrow \langle F_+ \rangle + \delta F_+$ where the noise-driven contribution at frequency $\omega \gg \omega_{\text{He}}, \Gamma_{\text{He}}$ is given by

$$\delta F_+(\omega) = \left(\gamma_e - \frac{\xi(\omega)\gamma_{\text{He}}}{\epsilon_N} \right) \frac{P_K N_K}{2} \frac{\delta B_+(\omega)}{\omega_K - \omega - i\Gamma_K} + W(\omega). \quad (10)$$

The first term describes the effect of magnetic field noise $\delta B_+ = \delta B_x + i\delta B_y$ at frequency ω when included in Eqs. (5-6) by $\mathbf{B} = \delta B_x \hat{\mathbf{x}} + \delta B_y \hat{\mathbf{y}} + B_z \hat{\mathbf{z}}$. It describes tilting of the total potassium spin that is driven by coupling of the electron spin to the magnetic field (with gyromagnetic ratio $\gamma_e = 2.8$ MHz/G, first term in Eq. 10), or to the transverse spin-exchange shift that is exerted by the tilted collective spin of the helium (with gyromagnetic-ratio $\gamma_{\text{He}} = 3.2$ kHz/G, second term in Eq. 10). The last term $W(\omega)$ denotes the technical noise originating primarily from measurement of the probe beam.

In Fig. 3 we exemplify the noise characteristics of the detector by presenting the square root of the power spectral density (PSD) of two recordings using Welch's method. The recordings were taken at two different magnetic fields $B_z = 19$ mG (pink circles) and $B_z = 50$ mG (brown circles) for 5 seconds each. The two noise spectra are presented in the raw units of the measuring device. The detector response to transverse oscillating magnetic-fields at these conditions are independently measured, and shown with dashed, and dotted-dashed lines respectively. We find an approximately white magnetic noise floor of about ~ 10 fT/ $\sqrt{\text{Hz}}$ accompanied with several narrow spikes, and also technical noise floor of about ~ 2 fT/ $\sqrt{\text{Hz}}$. The magnetic noise is consistent with the estimated noise produced by our innermost magnetic shield in the cell location [72], and is the limiting noise of our near-resonance measurement at most frequencies. The technical noise variance determines the realized sensitivity of our detector; It is proportional to the power of the probe beam and is considered as spin-independent because it is almost unchanged by turn off of the pump beam.

C. Calibrations

We have routinely calibrated the slowing down factor q by measurement of the EPR frequency as a function of B_z . The slope of the linear fit yields the gyromagnetic ratio of the polarized potassium which corresponds to γ_e/q .

We estimated the spin-exchange field produced by the helium spins using the measured data as detailed in the

data processing section. This estimation was validated by a measurement of the EPR the frequency during the spin-exchange optical-pumping stage (several hours process, preceded by application of strong magnetic fields that zeroed the initial helium polarization). We fitted it to the function

$$\omega_K(t) = \omega_K(0) + A_{\text{He}} P_{\text{He}}(1 - e^{-t/\tau}). \quad (11)$$

We calibrated the sensitivity of the magnetometer to weakly oscillating magnetic fields at the beginning and at the end of every measurement round, in between changes of the magnetic field value. We applied an additional calibration field $B = B_0 \cos(\omega_y t) \hat{y}$ with amplitude $B_0 = 2.7 \mu\text{G}$, and measured the response for several ω_y sampled around the EPR resonance. This measurement enabled the construction of the spectral form of the response function. The width and calibration factor remained very stable ($< 10\%$ drift) during a single measurement. The EPR resonance however was decreased during the measurement because of temporal change in $P_{\text{He}}(t)$; While the helium spins were polarized at $B = 70 \text{ mG}$ at the onset of each measurement, at lower magnetic fields the decoherence of the helium spins rate was moderately increased, primarily due to spatial inhomogeneity in the alkali-metal spins polarization [54]. The temporal variation in the spin-exchange field which shifted the EPR frequency was included in the analysis.

D. Data processing

We analyzed the data using the log-likelihood ratio test to exclude the presence of ALPs at frequency ω_{DM} with a width determined by the signal coherence time and the effects of earth's rotation on the sensitive axes of the detector. To accurately account for the velocity distribution of the Dark Matter, we carried the analysis procedure that is similar to Ref. [11] except for a few changes listed below. In short, we take the total ALP field as a superposition of the plane-waves representing the individual particles, whose momentum distribution follows the Standard Halo Model [42] and phases are uncorrelated and randomly distributed. To calculate the signal generated by the total ALP gradient, we compute the response of the detector in the frequency domain (which is represented by the α matrices as defined in Ref. [11]). Once the spectral content of an ALP has been determined, we use frequencies outside the predicted spectral content of the ALP to estimate the level of noise for the white noise hypothesis used to generate the bounds.

All analysis procedures and cuts were designed in a blind fashion, and decided in advance before looking at the data, to eliminate bias. We emphasize that this is an exclusion search, and no discovery was attempted. We carried a similar procedure for the quality cuts as described in Ref. [11], primarily to avoid a change in the analysis procedure, which presumably mitigated low-frequency noise; Indeed the noise spectrum of the unblinded data was nearly unchanged. We also note that owing to the long measurement time, spectral representation of the ALP required fewer points than in Ref. [11], rendering its computation more efficient.

The magnetization of the helium has decayed during the measurement, owing to its magnetic-field dependent lifetime. This rendered both ξ and ω_K time-dependent, slowly-varying throughout the measurement at the scale of many minutes. Because this time scale is much longer than $1/\omega_{\text{DM}}$, we assumed that P_{He} , and ω_K change adiabatically, such that Eqs. (3-7) remain valid at short time scales. We first classified if a decay is negligible based on the following criterion: we compared the EPR frequencies of the magnetic-response function measured at the calibration preceding and appending the recording and checked for variation that is greater than 200 Hz. This criterion classified most runs with $\omega_K(B_z) \gtrsim 20 \text{ kHz}$ as cases with negligible decay, where we took the average of the two EPR frequencies and the average of helium polarizations as constant values (note that in this regime $\Gamma_K \gtrsim 800 \text{ Hz}$). For the other cases, we have estimated the spin-exchange field of the helium spins as a function of time; we computed the spectrum of the data in a window of about one second every few seconds, and fitted it to an amalgam of the response functions (taken during the calibration stages) whose central frequency follows the central peak of the noise spectrum. Because the fitting function is several orders of magnitude wider in frequency than ALP signals, this procedure introduces no bias to the search. The time-dependence of the response was then used in computation of α (see [11]).

-
- [1] P. Zyla *et al.* (Particle Data Group), Review of Particle Physics, [PTEP 2020, 083C01 \(2020\)](#).
 - [2] W. Hu, R. Barkana, and A. Gruzinov, Cold and Fuzzy Dark Matter, [Phys. Rev. Lett. 85, 1158 \(2000\)](#), [arXiv:astro-ph/0003365 \[astro-ph\]](#).
 - [3] R. D. Peccei and H. R. Quinn, CP Conservation in the presence of pseudoparticles, [Physical Review Letters 38, 1440 \(1977\)](#).
 - [4] S. Weinberg, A new light boson?, [Physical Review Letters 40, 223 \(1978\)](#).
 - [5] F. Wilczek, Problem of Strong P and TInvariance in the presence of instantons, [Physical Review Letters 40, 279 \(1978\)](#).

- [6] C. B. Adams *et al.*, Axion Dark Matter, in *2022 Snowmass Summer Study (2022)* [arXiv:2203.14923 \[hep-ex\]](#).
- [7] M. Safronova, D. Budker, D. DeMille, D. F. J. Kimball, A. Derevianko, and C. W. Clark, Search for new physics with atoms and molecules, *Reviews of Modern Physics* **90**, 025008 (2018).
- [8] P. W. Graham, I. G. Irastorza, S. K. Lamoreaux, A. Lindner, and K. A. van Bibber, Experimental searches for the axion and axion-like particles, *Annual Review of Nuclear and Particle Science* **65**, 485 (2015).
- [9] M. Battaglieri *et al.*, US Cosmic Visions: New Ideas in Dark Matter 2017: Community Report, in *U.S. Cosmic Visions: New Ideas in Dark Matter* (2017) [arXiv:1707.04591 \[hep-ph\]](#).
- [10] A. V. Gramolin, A. Wickenbrock, D. Aybas, H. Bekker, D. Budker, G. P. Centers, N. L. Figueroa, D. F. J. Kimball, and A. O. Sushkov, Spectral signatures of axionlike dark matter, *Physical Review D* **105**, 035029 (2022).
- [11] I. M. Bloch, G. Ronen, R. Shaham, O. Katz, T. Volansky, and O. Katz, New constraints on axion-like dark matter using a floquet quantum detector, *Science advances* **8**, eabl8919 (2022).
- [12] I. M. Bloch, Y. Hochberg, E. Kufflik, and T. Volansky, Axion-like relics: new constraints from old comagnetometer data, *Journal of High Energy Physics* **2020**, 1 (2020).
- [13] A. Banerjee, D. Budker, J. Eby, V. V. Flambaum, H. Kim, O. Matsedonskyi, and G. Perez, Searching for earth/solar axion halos, *Journal of High Energy Physics* **2020**, [10.1007/jhep09\(2020\)004](#) (2020).
- [14] C. P. Salemi (ABRACADABRA), First Results from Abracadabra-10Cm: a Search for Low-Mass Axion Dark Matter, in *54Th Rencontres De Moriond on Electroweak Interactions and Unified Theories (Moriond Ew 2019) La Thuile, Italy, March 16-23, 2019* (2019) [arXiv:1905.06882 \[hep-ex\]](#).
- [15] A. Garcon, D. Aybas, J. W. Blanchard, G. Centers, N. L. Figueroa, P. W. Graham, D. F. J. Kimball, S. Rajendran, M. G. Sendra, A. O. Sushkov, *et al.*, The cosmic axion spin precession experiment (casper): a dark-matter search with nuclear magnetic resonance, *Quantum Science and Technology* **3**, 014008 (2017).
- [16] W. A. Terrano, E. G. Adelberger, C. A. Hagedorn, and B. R. Heckel, Constraints on axionlike dark matter with masses down to 10^{-23} eV/c², *Phys. Rev. Lett.* **122**, 231301 (2019), [arXiv:1902.04246 \[astro-ph.CO\]](#).
- [17] P. W. Graham, D. E. Kaplan, J. Mardon, S. Rajendran, W. A. Terrano, L. Trahms, and T. Wilkason, Spin Precession Experiments for Light Axionic Dark Matter, *Phys. Rev. D* **97**, 055006 (2018), [arXiv:1709.07852 \[hep-ph\]](#).
- [18] A. Garcon *et al.*, Constraints on bosonic dark matter from ultralow-field nuclear magnetic resonance, *Sci. Adv.* **5**, eaax4539 (2019), [arXiv:1902.04644 \[hep-ex\]](#).
- [19] T. Wu *et al.*, Search for Axionlike Dark Matter with a Liquid-State Nuclear Spin Comagnetometer, *Phys. Rev. Lett.* **122**, 191302 (2019), [arXiv:1901.10843 \[hep-ex\]](#).
- [20] K. M. Backes, D. A. Palken, S. A. Kenany, B. M. Brubaker, S. B. Cahn, A. Droster, G. C. Hilton, S. Ghosh, H. Jackson, S. K. Lamoreaux, A. F. Leder, K. W. Lehnert, S. M. Lewis, M. Malnou, R. H. Maruyama, N. M. Rapidis, M. Simanovskaia, S. Singh, D. H. Speller, I. Urdinaran, L. R. Vale, E. C. van Assendelft, K. van Bibber, and H. Wang, A quantum enhanced search for dark matter axions, *Nature* **590**, 238 (2021).
- [21] M. Jiang, H. Su, A. Garcon, X. Peng, and D. Budker, Search for axion-like dark matter with spin-based amplifiers (2021), [arXiv:2102.01448 \[hep-ph\]](#).
- [22] P. Vorob'ev and I. Kolokolov, Detectors for the cosmic axionic wind, *arXiv preprint astro-ph/9501042* (1995).
- [23] D. J. Kimball, Nuclear spin content and constraints on exotic spin-dependent couplings, *New Journal of Physics* **17**, 073008 (2015).
- [24] C. Abel *et al.*, Search for Axionlike Dark Matter Through Nuclear Spin Precession in Electric and Magnetic Fields, *Phys. Rev. X* **7**, 041034 (2017), [arXiv:1708.06367 \[hep-ph\]](#).
- [25] G. Vasilakis, J. M. Brown, T. W. Kornack, and M. V. Romalis, Limits on New Long Range Nuclear Spin-Dependent Forces Set with a K - He-3 Co-Magnetometer, *Phys. Rev. Lett.* **103**, 261801 (2009), [arXiv:0809.4700 \[physics.atom-ph\]](#).
- [26] G. P. Centers *et al.*, Stochastic fluctuations of bosonic dark matter, *Nature Commun.* **12**, 7321 (2021), [arXiv:1905.13650 \[astro-ph.CO\]](#).
- [27] M. Bulatowicz, R. Griffith, M. Larsen, J. Mirijanian, T. G. Walker, C. B. Fu, E. Smith, W. M. Snow, and H. Yan, A Laboratory Search for a Long-Range T-odd, P-odd Interaction from Axion-Like Particles using Dual Species Nuclear Magnetic Resonance with Polarized Xe-129 and Xe-131 Gas, *Phys. Rev. Lett.* **111**, 102001 (2013), [arXiv:1301.5224 \[physics.atom-ph\]](#).
- [28] S. S. Sorensen, D. A. Thrasher, and T. G. Walker, A synchronous spin-exchange optically pumped nmr-gyroscope, *Applied Sciences* **10**, 10.3390/app10207099 (2020).
- [29] T. R. Gentile, P. J. Nacher, B. Saam, and T. G. Walker, Optically Polarized ³He, *Rev. Mod. Phys.* **89**, 045004 (2017), [arXiv:1612.04178 \[physics.atom-ph\]](#).
- [30] Y. Wang, H. Su, M. Jiang, Y. Huang, Y. Qin, C. Guo, Z. Wang, D. Hu, W. Ji, P. Fadeev, *et al.*, Limits on axions and axionlike particles within the axion window using a spin-based amplifier, *Physical Review Letters* **129**, 051801 (2022).
- [31] M. A. Humphrey, D. F. Phillips, E. M. Mattison, R. F. Vessot, R. E. Stoner, and R. L. Walsworth, Testing cpt and lorentz symmetry with hydrogen masers, *Physical Review A* **68**, 063807 (2003).
- [32] J. Lee, M. Lisanti, W. A. Terrano, and M. Romalis, Laboratory constraints on the neutron-spin coupling of fev-scale axions, *arXiv preprint arXiv:2209.03289* (2022).
- [33] I. M. Bloch, Y. Hochberg, E. Kufflik, and T. Volansky, Axion-like Relics: New Constraints from Old Comagnetometer Data, *JHEP* **01**, 167, [arXiv:1907.03767 \[hep-ph\]](#).
- [34] M. Jiang, H. Su, Z. Wu, X. Peng, and D. Budker, Floquet maser, *Science Advances* **7**, eabe0719 (2021).
- [35] I. Kominis, T. Kornack, J. Allred, and M. V. Romalis, A subfemtotesla multichannel atomic magnetometer, *Nature* **422**, 596 (2003).
- [36] H. Dang, A. C. Maloof, and M. V. Romalis, Ultrahigh sensitivity magnetic field and magnetization measurements with an

- atomic magnetometer, *Applied Physics Letters* **97**, 151110 (2010).
- [37] O. Katz, M. Dikopoltsev, O. Peleg, M. Shuker, J. Steinhauer, and N. Katz, Nonlinear elimination of spin-exchange relaxation of high magnetic moments, *Physical review letters* **110**, 263004 (2013).
- [38] T. Wang, D. F. J. Kimball, A. O. Sushkov, D. Aybas, J. W. Blanchard, G. Centers, S. R. O’Kelley, A. Wickenbrock, J. Fang, and D. Budker, Application of spin-exchange relaxation-free magnetometry to the cosmic axion spin precession experiment, *Physics of the dark universe* **19**, 27 (2018).
- [39] G. G. Di Cortona, E. Hardy, J. P. Vega, and G. Villadoro, The qcd axion, precisely, *Journal of High Energy Physics* **2016**, 1 (2016).
- [40] J. E. Kim, Weak Interaction Singlet and Strong CP Invariance, *Phys. Rev. Lett.* **43**, 103 (1979).
- [41] M. A. Shifman, A. I. Vainshtein, and V. I. Zakharov, Can Confinement Ensure Natural CP Invariance of Strong Interactions?, *Nucl. Phys.* **B166**, 493 (1980).
- [42] S. K. Lee, M. Lisanti, and B. R. Safdi, Dark-matter harmonics beyond annual modulation, *Journal of Cosmology and Astroparticle Physics* **2013** (11), 033.
- [43] J. Ethier and W. Melnitchouk, Comparative study of nuclear effects in polarized electron scattering from ^3He , *Physical Review C* **88**, 054001 (2013).
- [44] I. M. Bloch, Nasduck serf bounds repository, <https://github.com/ItayBM/NASDUCKSERF> (2022).
- [45] E. G. Adelberger, B. R. Heckel, S. Hoedl, C. D. Hoyle, D. J. Kapner, and A. Upadhye, Particle-physics implications of a recent test of the gravitational inverse-square law, *Physical Review Letters* **98**, [10.1103/physrevlett.98.131104](https://doi.org/10.1103/physrevlett.98.131104) (2007).
- [46] A. Bhusal, N. Houston, and T. Li, Searching for solar axions using data from the sudbury neutrino observatory, *Physical Review Letters* **126**, [10.1103/physrevlett.126.091601](https://doi.org/10.1103/physrevlett.126.091601) (2021).
- [47] M. V. Beznogov, E. Rrapaj, D. Page, and S. Reddy, Constraints on Axion-like Particles and Nucleon Pairing in Dense Matter from the Hot Neutron Star in HESS J1731-347, *Phys. Rev.* **C98**, 035802 (2018), [arXiv:1806.07991](https://arxiv.org/abs/1806.07991) [astro-ph.HE].
- [48] K. Hamaguchi, N. Nagata, K. Yanagi, and J. Zheng, Limit on the axion decay constant from the cooling neutron star in cassiopeia a, *Physical Review D* **98**, [10.1103/physrevd.98.103015](https://doi.org/10.1103/physrevd.98.103015) (2018).
- [49] J. Keller and A. Sedrakian, Axions from cooling compact stars: Pair-breaking processes, *Nuclear Physics A* **897**, 62–69 (2013).
- [50] A. Sedrakian, Axion cooling of neutron stars, *Physical Review D* **93**, [10.1103/physrevd.93.065044](https://doi.org/10.1103/physrevd.93.065044) (2016).
- [51] J. H. Chang, R. Essig, and S. D. McDermott, Supernova 1987A Constraints on Sub-GeV Dark Sectors, Millicharged Particles, the QCD Axion, and an Axion-like Particle; Additional Private communications, *JHEP* **09**, 051, [arXiv:1803.00993](https://arxiv.org/abs/1803.00993) [hep-ph].
- [52] P. Carena, T. Fischer, M. Giannotti, G. Guo, G. Martínez-Pinedo, and A. Mirizzi, Improved axion emissivity from a supernova via nucleon-nucleon bremsstrahlung, *JCAP* **1910** (10), 016, [arXiv:1906.11844](https://arxiv.org/abs/1906.11844) [hep-ph].
- [53] N. Bar, K. Blum, and G. D’Amico, Is there a supernova bound on axions?, *Physical Review D* **101**, [10.1103/physrevd.101.123025](https://doi.org/10.1103/physrevd.101.123025) (2020).
- [54] O. Katz, R. Shaham, and O. Firstenberg, Coupling light to a nuclear spin gas with a two-photon linewidth of five millihertz, *Science advances* **7**, eabe9164 (2021).
- [55] T. G. Walker and W. Happer, Spin-exchange optical pumping of noble-gas nuclei, *Reviews of modern physics* **69**, 629 (1997).
- [56] O. Katz, O. Peleg, and O. Firstenberg, Coherent coupling of alkali atoms by random collisions, *Physical Review Letters* **115**, 113003 (2015).
- [57] W. Happer and A. Tam, Effect of rapid spin exchange on the magnetic-resonance spectrum of alkali vapors, *Physical Review A* **16**, 1877 (1977).
- [58] W. Happer and H. Tang, Spin-exchange shift and narrowing of magnetic resonance lines in optically pumped alkali vapors, *Physical Review Letters* **31**, 273 (1973).
- [59] A. Berrebi, M. Dikopoltsev, O. Katz, and O. Katz, Optical protection of alkali-metal atoms from spin relaxation, *arXiv preprint arXiv:2209.12360* (2022).
- [60] M. Dikopoltsev, A. Berrebi, U. Levy, and O. Katz, Suppressing the decoherence of alkali-metal spins at low magnetic fields, *arXiv preprint arXiv:2209.12236* (2022).
- [61] T. Kornack and M. Romalis, Dynamics of two overlapping spin ensembles interacting by spin exchange, *Physical review letters* **89**, 253002 (2002).
- [62] T. G. Walker and M. S. Larsen, Spin-exchange-pumped nmr gyros, in *Advances in atomic, molecular, and optical physics*, Vol. 65 (Elsevier, 2016) pp. 373–401.
- [63] R. Shaham, O. Katz, and O. Firstenberg, Strong coupling of alkali-metal spins to noble-gas spins with an hour-long coherence time, *Nature Physics* **18**, 506 (2022).
- [64] M. Lisanti, M. Moschella, and W. Terrano, Stochastic properties of ultralight scalar field gradients, *Phys. Rev. D* **104**, [055037](https://doi.org/10.1103/physrevd.104.055037) (2021), [arXiv:2107.10260](https://arxiv.org/abs/2107.10260) [astro-ph.CO].
- [65] G. Vasilakis, J. Brown, T. Kornack, and M. Romalis, Limits on new long range nuclear spin-dependent forces set with a ^3He comagnetometer, *Physical review letters* **103**, 261801 (2009).
- [66] J. M. Brown, S. J. Smullin, T. W. Kornack, and M. V. Romalis, New Limit on Lorentz and Cpt-Violating Neutron Spin Interactions, *Phys. Rev. Lett.* **105**, 151604 (2010), [arXiv:1006.5425](https://arxiv.org/abs/1006.5425) [physics.atom-ph].
- [67] M. Padniuk, M. Kopciuch, R. Cipolletti, A. Wickenbrock, D. Budker, and S. Pustelny, Response of atomic spin-based sensors to magnetic and nonmagnetic perturbations, *Scientific reports* **12**, 1 (2022).
- [68] T. Kornack, S. Smullin, S.-K. Lee, and M. Romalis, A low-noise ferrite magnetic shield, *Applied physics letters* **90**, 223501 (2007).

- [69] W. Happer, Y. Jau, and T. Walker, *Optically Pumped Atoms* (Wiley, 2010).
- [70] S. Appelt, A. B.-A. Baranga, C. Erickson, M. Romalis, A. Young, and W. Happer, Theory of spin-exchange optical pumping of ^3He and ^{129}Xe , *Physical review A* **58**, 1412 (1998).
- [71] O. Katz, R. Shaham, and O. Firstenberg, Quantum interface for noble-gas spins based on spin-exchange collisions, *PRX quantum* **3**, 010305 (2022).
- [72] S.-K. Lee and M. Romalis, Calculation of magnetic field noise from high-permeability magnetic shields and conducting objects with simple geometry, *Journal of Applied Physics* **103**, 084904 (2008).